



Phosphate modified ZSM-5 for the shape-selective synthesis of *para*-diethylbenzene: Role of crystal size and acidity



Janardhan L. Hodala, Anand B. Halgeri, Ganapati V. Shanbhag*

Materials Science Division, Poornaprajna Institute of Scientific Research (PPISR), Bidalur Post, Devanahalli, Bengaluru 562110, India

ARTICLE INFO

Article history:

Received 28 April 2014

Received in revised form 23 June 2014

Accepted 4 July 2014

Available online 12 July 2014

Keywords:

Phosphate modification

Shape selectivity

Zeolite

ZSM-5

Alkylation

Vapor phase

p-diethylbenzene

ABSTRACT

Pore engineered ZSM-5 zeolite in extrudate form was prepared and used as shape-selective catalyst for vapor phase ethylation of ethylbenzene to selectively form *para*-diethylbenzene. The physico-chemical properties of the catalyst were established by XRD, N₂ sorption, FTIR, FESEM, NH₃-TPD and ³¹P MAS NMR. Alkylation of ethylbenzene with ethanol was carried out in a continuous, down-flow, tubular reactor, at atmospheric pressure and H₂ as a carrier gas in vapor phase. Effect of silica to alumina ratio (SAR), crystal size, acidity of phosphate modified ZSM-5, stepwise phosphate modification and reaction conditions were studied in detail. ZSM-5 with SAR 187 was found to contain optimum acidity for phosphate modification to achieve good conversion and high selectivity for *p*-diethylbenzene. Under optimized reaction conditions, viz. temperature = 380 °C, ethylbenzene:ethanol mole ratio = 4:1, WHSV = 3 h⁻¹, H₂/reactants = 2, 5PZSM-5 W catalyst gave 22.8% of ethylbenzene conversion with ~98% selectivity for *para*-diethylbenzene.

© 2014 Elsevier B.V. All rights reserved.

1. Introduction

Zeolites (microporous crystalline aluminosilicates) have been widely used as eco-friendly catalysts, and have successfully replaced corrosive and environmentally unsafe catalysts. They exhibit shape-selectivity for the chemical reactions due to their microporous channels [1] and are applied for selective organic transformations. To enhance the selectivity for the desired product, pores of zeolites are regulated and usually done by post synthesis modification. Silica deposition on the external surface, metal/non metal oxide impregnation and controlled coking are widely applied as post synthesis methods to regulate pore size [2–8]. Phosphate impregnation on ZSM-5 is one such method studied by several groups [9–21] but the studies were mainly restricted to the shape selective synthesis of *p*-xylene from alkylation of toluene with methanol and physico-chemical changes of zeolite ZSM-5 after phosphate modification. Recently, Janardhan et al. reported the effect of generation of new acid sites and effect of water treatment on phosphate modified ZSM-5, which showed remarkable improvement in shape selectivity while retaining good activity [22]. *p*-Diethylbenzene (PDEB) is an important chemical used as

a desorbent in PAREX process designed by UOP. In PAREX process, *p*-xylene is separated from its regioisomers and used as a raw material for polyester synthesis such as PET and PTA. Ethylation of ethylbenzene over acidic catalysts in vapor phase gives thermodynamic equilibrium mixtures of *o,m,p*-diethylbenzenes. A high purity PDEB is required for PAREX process, which can be synthesized by the reduction of *p*-ethylacetophenone, known to be an expensive multistep process. Hence, it is necessary to design a selective catalyst for ethylation of ethylbenzene which forms only *para* isomer. Few research groups have reported catalysts like silica coated ZSM-5, ZSM-5 impregnated with lanthanum and cerium oxides, aluminophosphates, phosphotungstic acid supported on aluminophosphates AlPO and modified zeolites to selectively synthesize PDEB from ethylation of ethylbenzene with ethanol or ethylene [23–31]. Halgeri and co-workers had extensively worked on silanation of ZSM-5 for the synthesis of PDEB by ethylation of ethylbenzene [28–31]. Unlike other methods, phosphate modification is an easy and inexpensive route for the catalyst modification, which makes it a good prospect for a commercial process.

Only few studies have been reported on alkylation of ethylbenzene and benzene with ethanol/ethylene over phosphate treated ZSM-5 for selective synthesis of PDEB [11,18]. In these reports, activities of the catalysts reported were very low and hence high concentrations of alkylating agent were used. These catalysts contained ionic phosphates in the channels, which created diffusion problems [22].

* Corresponding author. Tel.: +91 80 27408552; fax: +91 80 23611836.

E-mail addresses: shanbhag@poornaprajna.org, gvshanbhag@yahoo.co.in
(G.V. Shanbhag).

In previous study, the authors showed that water treatment after phosphate impregnation and calcination of ZSM-5 remarkably enhances the activity while retaining product selectivity with probe reactions viz. toluene methylation, ethylbenzene ethylation and disproportionation, and competitive reaction of *m*-xylene and ethylbenzene [22]. In the present article, detailed studies on role of crystal size of ZSM-5 and acidity of water treated phosphate modified ZSM-5 was carried out for ethylbenzene alkylation with ethanol reaction. Effect of different operating parameters on the conversion and product selectivity was also studied in detail.

2. Experimental

2.1. Catalyst preparation

Zeolite ZSM-5 with different silica to alumina ratios (SAR) were kindly donated by Süd-Chemie India Pvt Ltd. Sodium form of zeolites were exchanged with ammonium ions by refluxing in 1 M aq. NH_4NO_3 solution for 4 h, filtered and dried, and this procedure was repeated twice to ensure maximum ion-exchange. The final product was calcined at 550 °C for 3 h to get HZSM-5. Further, HZSM-5 was modified post synthetically by wet impregnation method by treatment with phosphorus reagent. In step 1, required amount of $\text{NH}_4\text{H}_2\text{PO}_4$ was dissolved in 22 ml water at 60 °C to which 5 g of zeolite was added with stirring and evaporated at 90 °C. It was then dried at 120 °C for 4 h and calcined initially at 330 °C for 3 h and then the temperature was increased to 560 °C for 10 h. This calcined catalyst powder was cooled to room temperature and stirred in water at 80 °C for 12 h, then filtered and dried at 120 °C for 4 h (Step 2). In step 3, it was then extruded with silica binder (Ludox AS 40), dried in an oven for 4 h at 120 °C and calcined at 500 °C for 8 h. Thus prepared catalysts were designated as XPZSM-5W where X is percentage of P (as phosphate) added during impregnation and W is the water treatment after P impregnation and calcination.

Another set of catalysts were prepared by two-step addition of phosphates. For this, the procedure followed was similar to the previously mentioned one except that phosphate impregnation was repeated once after Step 2. Catalyst prepared were 1 + 4PZSM-5 W, 2 + 3PZSM-5 W, 3 + 2PZSM-5 W (a + bPZSM-5 W, where a = % P added during first step, b = % P added during second step).

2.2. Catalyst characterization

X-ray diffraction studies were performed with Bruker D2 Phaser diffractometer equipped with Cu K α source. X-ray diffraction data collected was from 5° to 50° Bragg angle with steps of 0.02 with an interval of 0.5 s. FTIR spectra were obtained on Bruker Alpha instrument in ATR mode. Spectral data were collected from 500 to 1500 cm⁻¹ with a resolution of 4 cm⁻¹ and average of 32 scans. Nitrogen sorption measurements were carried out over Autosorb-1 C (Quantachrome, USA) unit. The isotherms were measured at 77 K after degassing samples below 10⁻³ Torr at 300 °C for 4 h. The BET specific surface area was estimated using adsorption data as per the ASTM 4365 method applicable for microporous solids. The total pore volume was estimated from the amount adsorbed at a relative pressure of about 0.95. The acidity of the catalysts was measured by temperature programmed desorption (TPD) of NH₃. In a typical procedure, 0.1 g of sample was taken in a quartz tube of 1/4 in. packed with silica wool from both sides to remove dead volume and sample was dehydrated at 550 °C for 1 h. The temperature was decreased to 100 °C and NH₃ was adsorbed by passing a stream of 10% NH₃ in He through catalyst bead for 1 h. Physisorbed NH₃

was then purged by dry He for another 1 h. The desorption of NH₃ was carried out in He flow (30 ml min⁻¹) by increasing the temperature to 550 °C at 10 °C min⁻¹ using TCD detector. Point of zero charge (PZC) was determined by mass titration method. In a typical procedure, 3 g of catalyst was added in multiples of 200 mg of catalyst to 100 ml of 0.1 M KCl solution with stirring. The pH was measured (with calibrated digital pH meter) each time after adding 200 mg catalyst and 30 min of equilibrium. PZC was determined from the plot of pH v/s catalyst weight. That pH value is considered as PZC, after which, addition of the catalyst to the solution has negligible effect on pH [32]. Solid state nuclear magnetic resonance with magic angle spinning (MAS NMR) was performed in Bruker DSX 300 using standard procedure. Sample was placed in a 4 mm probe and was spun at 5 KHz. Chemical shifts were plotted with respect to reference standards, $\text{NH}_4\text{H}_2\text{PO}_4$ and $\text{Al}(\text{NO}_3)_3$ for ³¹P and ²⁷Al nuclei respectively. Phosphorus content in the modified catalyst was estimated by colorimetry [33]. In a typical procedure, catalyst was digested with a mixture of 1 g of HCl, 0.5 g HF and 1 g HNO_3 . The mixture was then neutralized with H_3BO_3 and this mixture was diluted to 200 ml. 2 ml of this solution was taken in 50 ml volumetric flask and 5 ml of 2 M H_2SO_4 was added followed by 5 ml of 0.01 M ammonium paramolybdate. To this solution, 4 ml of mixed reagent (1:1 mixture of freshly prepared 10% ascorbic acid: 0.004 M antimony potassium tartrate solution) was added to get intense blue color. After 10 min, optical density (OD) was measured at 890 nm in PerkinElmer UV-Vis spectrophotometer. Similar method was followed to make $\text{NH}_4\text{H}_2\text{PO}_4$ standard solutions and phosphorus was estimated in the catalyst samples using 5 point calibration curve obtained from standard solutions. Morphology of the catalysts were studied with FESEM. In a typical procedure, a small amount of catalyst was smeared on carbon tape glued to the stage, degassed in vacuum for 24 h, sputtered with gold for 1 min and image was collected in Zeiss instrument with different magnifications.

Coke was estimated by calcination of spent catalyst in air to get constant weight (till the coke was completely removed). Difference in weight before and after calcinations is considered as amount of coke formed during reaction. It was normalized to hundred and expressed in terms of percentage coke formed.

2.3. Catalyst evaluation with alkylation of ethylbenzene with ethanol

Ethylbenzene ethylation was carried out in a vapor phase continuous down-flow quartz reactor. Quartz reactor was connected to a preheater at ~250 °C and a condenser maintained at 2 °C with the help of cryostat. About 2 g of extruded, calcined catalyst of 3–6 mm length and 1.5 mm Ø was taken in the quartz reactor. Internal diameter of the reactor was 14 mm and ratio of the reactor diameter to catalyst diameter was always in the range of 9–10. Catalyst bed was spread evenly with ceramic beads on the top and a thermocouple to sense the bed temperature. It was then placed inside the furnace and heated to a desired temperature. In a typical procedure, catalyst was activated *in-situ* at 500 °C for 1 h in air before reaction and reaction temperature was set to 380 °C. A mixture of ethylbenzene and ethanol was taken with 4:1 mol ratio and fed into the preheater at a required rate through a syringe pump (New Era pump system Inc). Carrier gas was fed through the calibrated rotameter. Gaseous product stream was condensed and collected in gas liquid separator maintained at 2–5 °C. Liquid and gas products were analyzed (off-line) through GC using HP-Innowax capillary column; 60 m × 0.25 µm × 0.25 mm and porapak Q packed column; 4 m × 200 mm respectively. The components were identified and quantified with standards, and confirmed by GCMS.

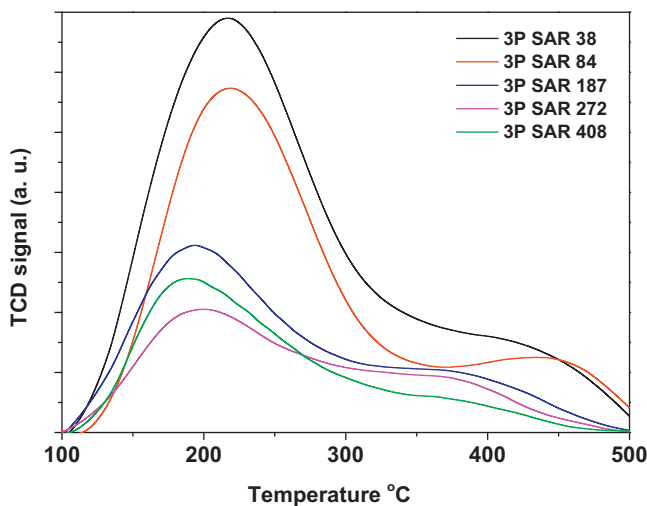


Fig. 1. TPD of ammonia trace and acidity of 3PZSM-5W with different SAR.

3. Results and discussion

3.1. Catalyst characterization

XRD patterns of unmodified HZSM-5 matched well with all phosphate modified samples. This showed the retention of structural integrity of ZSM-5 after phosphate modification followed by water treatment (Figs. S1, S2A and S3). It is further confirmed by the IR spectrum that the bands corresponding to pentasil chain (at 1220–1230 cm⁻¹) and pentasil unit (at 540–550 cm⁻¹) did not shift positions as compared with zeolite without modification (Figs. S2B, S4, S5 and S6).

Surface area of PZSM-5 after phosphate modification decreased (Table S1) from 525 to 368 m²/g which could be due to the impregnated phosphate groups occupied both in external and micropore areas. Surface area was completely restored after 1% P loading and subsequent water treatment whereas at higher loadings, surface area decreased by ~30%. Pore volume after phosphate modification also decreased marginally.

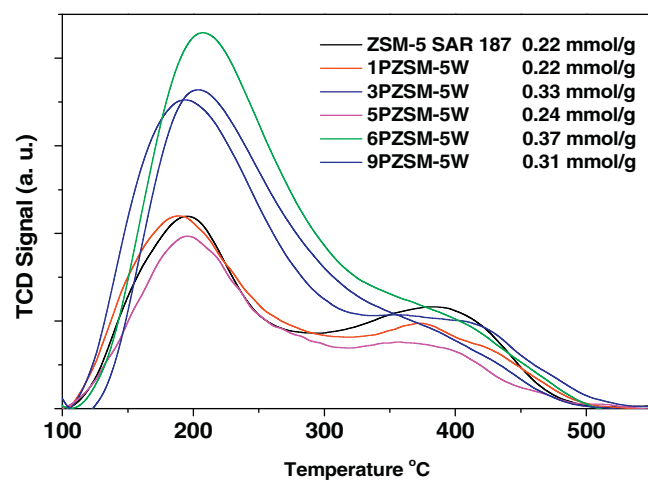


Fig. 2. TPD of ammonia trace and acidity of phosphate modified ZSM-5.

TPD of ammonia showed that the stronger acid sites were replaced with weaker acid sites after phosphate modification (Figs. 1 and 2). It is evident that the phosphate salt reacts with the acid sites creating new kinds of acid (active) sites. Interestingly, it is evident from the TPD plot that stronger acid sites decreased after phosphate modification but total acidity marginally changed (Tables 1–3).

Nitrogen sorption shows the decrease in surface area and pore volume after P-modification at phosphate loadings >1%. TPD of ammonia analysis of P-modified and unmodified zeolite samples shows a marginal change in the acidity of zeolite. The shift of peaks at lower temperatures showed that stronger acid sites were killed after P-modification.

Point of Zero Charge (PZC) measurement gives the information regarding the surface coverage [29]. The plot of PZC vs wt% of phosphate on ZSM-5 shows a break at monolayer coverage. This break was observed at 4% P loading, indicating the completion of monolayer islands formation at this loading. Phosphates added were chemisorbed to form monolayer to multilayer. Better performance of the catalyst can be achieved at monolayer formation because

Table 1
Acidity, P-content and activity studies of PZSM-5 with different crystal sizes.

Morphology and average crystal size μm	SAR	Acidity (mmol/g)	P added (wt%)	P remaining after water treatment (wt%)	Acidity After water P modification (mmol/g)	P/Al	^a EB Conversion (wt%)	^a Benzene selectivity (wt%)	DEB Selectivity (wt%)	^a PDEB selectivity (wt%)
Spherical 0.63	240	0.22	0	–	n/a	–	35.6	12.9	85.1	38.6
			2	0.45	0.29	0.47	27.7	8.1	86.1	53.5
			5	0.94	0.30	0.98	23.7	7.8	88.4	88.3
Irregular 1.2	272	0.19	0	–	n/a	–	16.7	3.6	98.9	66.13
			2	0.51	0.29	0.60	23	3.5	97.3	80.4
			5	1.05	0.16	1.24	20.3	3.4	95.5	98.4
Cuboid 1.1#	280	0.20	0	–	n/a	–	16.3	6.6	91.5	62.7
			2	0.40	0.17	0.39	15.5	6.3	91.4	72.1
			5	1.01	0.18	0.99	13.5	5.2	92.5	91.5
Inter grown cube 3.9	250	0.24	0	–	n/a	–	25.7	10.9	86	61.4
			2	0.45	0.28	0.49	19.9	10.4	84	87.1
			5	1.02	0.19	1.11	16.1	10.0	88	97.6

^a Conditions: temperature = 380 °C WHSV = 3 h⁻¹, catalyst weight = 2 g, H₂: reactants = 2, ethylbenzene:ethanol = 4:1, time = 4 h; # based on volume equivalent sphere diameter.

Table 2

Acidity and P-content of PZSM-5 with different SAR.

HZSM-5 (SAR)	HZSM-5 acidity (mmol/g)	P added (wt%)	P remaining water treatment (wt%)	Acidity after water treatment (mmol/g)	P/Al
38	1.74	3	1.78	0.76	0.29
84	1.5	3	0.88	0.48	0.32
187	0.22	3	0.89	0.33	0.72
272	0.19	3	0.92	0.21	1.09
408	0.17	3	0.87	0.21	1.55

Table 3

Stepwise phosphate modification of HZSM-5 (SAR-187).

Catalyst	Step 1 P added (wt%)	Step 2 P added (wt%)	P remaining after water treatment (wt%)	Acidity after water treatment (mmol/g)	P/Al	^a EB conversion (wt%)	^a Ethanol conversion (wt%)	^a PDEB selectivity (wt%)
HZSM-5	0	0	0	0.22	–	17.3	99.9	70
1 + 4PZSM 5W	1	4	0.66	0.20	0.54	21	99.9	97
2 + 3 PZSM-5W	2	3	0.90	0.28	0.94	21	99.9	97
3 + 2PZSM-5W	3	2	0.66	0.20	0.54	21	99.9	97
5 PZSM-5W	5	0	0.81	0.24	0.66	22.8	99.9	98.5

^a Conditions: temperature = 380 °C WHSV = 3 h⁻¹, catalyst weight = 2 g, H₂: reactants = 2, ethylbenzene:ethanol = 4:1, time = 4 h.

higher loadings result in multilayer of phosphates which may block the pores to create diffusion problems [22].

The % of phosphorus added during preparation was plotted with phosphorus remaining after water treatment. In all the preparations of PZSM-5 catalysts, phosphate to aluminium mole ratio added was >1. The plot shows that, as the phosphate impregnation increased from 0 to 3%, phosphate content in zeolite after water treatment increased linearly and becomes almost constant at 0.8–0.9% up to 6% impregnation [22]. This shows the saturation of phosphate monolayer islands inside the pores. At higher phosphate impregnations (>6%), there is an increase in phosphate content which may be due to the formation of multilayer of phosphates. These monolayer phosphate sites catalyze the reaction and increase the selectivity by imparting additional diffusion barrier to formed isomers.

²⁷Al MAS NMR (Fig. 3(A and B)) spectra confirm that all the Al are tetrahedral in nature in both ZSM-5 (SAR 187) and 5PZSM-5 W (SAR 187). This indicates that Al sites are retained in the zeolite framework after phosphate modification and dealumination did not occur. Interestingly, the peak at 53.3 ppm corresponding to framework Al shifted downfield marginally to 56.5 ppm after phosphate treatment. This could be due to phosphate and framework Al interactions as shown in Scheme 1. ³¹P MAS NMR spectra of PZSM-5W showed pyrophosphate, polyphosphate, and aluminophosphate species (-5.72, -22.05, -32.87 ppm respectively) (Fig. 3(C)). This shows that orthophosphate interaction with zeolite matrix. However, pyrophosphate, polyphosphate, and aluminophosphate formed a stable interaction with the zeolite hence it was retained even after water treatment. Similar observation for water treated PZSM-5 was reported by Derewinski et al. [34]. There

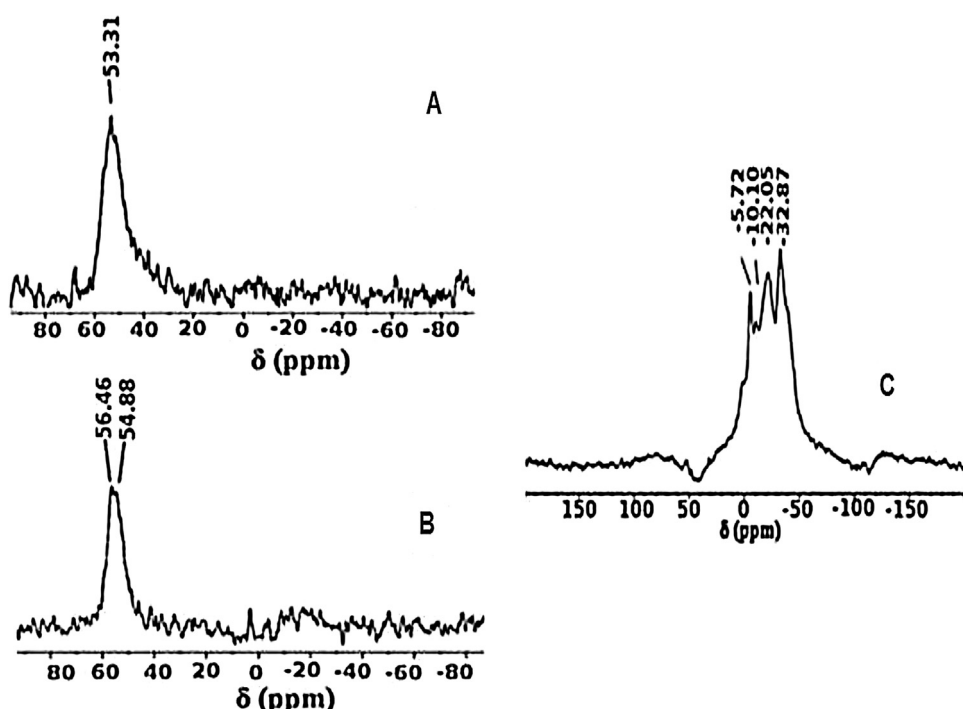
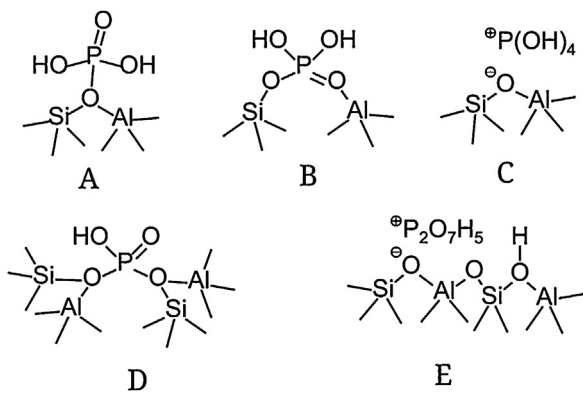


Fig. 3. ²⁷Al MAS NMR of (A) ZSM-5, (B) 5PZSM-5W, (C) ³¹P MAS NMR of 5PZSM-5-W.



Scheme 1. Phosphate interaction with zeolite framework as adopted from A [12], B [37], C [15], D [38], E [15].

was no aggregation or change in morphology for 5PZSM-5 W contrary to the observations made by the van der Bij et al. where water treatment was not carried out [35]. Morphologies of the catalysts before and after modification were spherical with particle size in the range of 1.5–3.1 μm (Fig. 4(A and B)).

To understand the effect of acidity on phosphate modification, 3PZSM-5 W catalysts with different SAR were prepared and characterized for phosphate content and acidity by TPD of ammonia. For unmodified HZSM-5 catalysts, acidity decreased with increase in SAR as expected (Fig. 1, Table 2). After P-modification, phosphates per Al site increased with increase in SAR even though phosphate added to the zeolite was constant (3 wt%). It could be attributed to the interaction of phosphates predominantly with Al sites at lower SAR and increase in SAR increases phosphate-phosphate interactions forming poly-phosphates. Phosphorus retained on zeolite was almost constant for all SAR except SAR 38. Interestingly, the acidity of ZSM-5 increased for higher SAR of 187, 272, 408 after phosphate treatment. The increase in acidity after modification could be due

to generation of new kind of low strength acid sites [22]. In previous reports, ZSM-5 with lower SAR < 100 were used invariably for preparing PZSM-5 and reported decrease in acidity after modification. In present study, decrease in acidity after P-modification is true only for ZSM-5 with low SAR and interestingly, marginal increase acidity was observed for higher SAR. This change in acidity can be explained with respect to the possible modes of interaction of phosphates with zeolite framework as shown in Scheme 1 (adopted from Refs. [12,15,37,38]). At lower SAR, possibility of formation of structures C and D is relatively high due to high acid site density. For higher SAR, formation of A and B is possible due to well dispersed acid sites which results in the formation of two acid sites by replacing one acid site and hence acidity increased. Formation of species C, D, and E result in decrease of acid sites. ³¹P MAS NMR spectra of 5PZSM-5W (SAR 187) suggests that all 5 species can form but relative change in acidity can possibly be attributed to relative abundance of these species over PZSM-5 with different SAR.

During 2-step phosphate addition, phosphates retained was almost similar for all catalysts except 2+3 PZSM-5 which showed maximum phosphorus retention of 0.9% (0.94 P/Al) (Table 3, Fig S7). Some Al sites which left unreacted during first step addition may react with phosphates during second step. However, the reaction of phosphate groups formed during the first step with phosphates added in the second step cannot be ruled out. Acidity of different PZSM-5W prepared with 2-step phosphate additions were in the range 0.20–0.28 mmol H⁺/g whereas unmodified HZSM-5 showed acidity of 0.22 mmol H⁺/g.

3.2. Alkylation of ethylbenzene with ethanol

Alkylation of ethylbenzene with ethanol in a continuous down-flow reactor in vapor phase gives mainly a mixture of *o,m,p*-diethylbenzenes (hereafter DEB). Minor products such as benzene, toluene, xylene, ethyltoluene, triethylbenzene were also formed during the reaction.

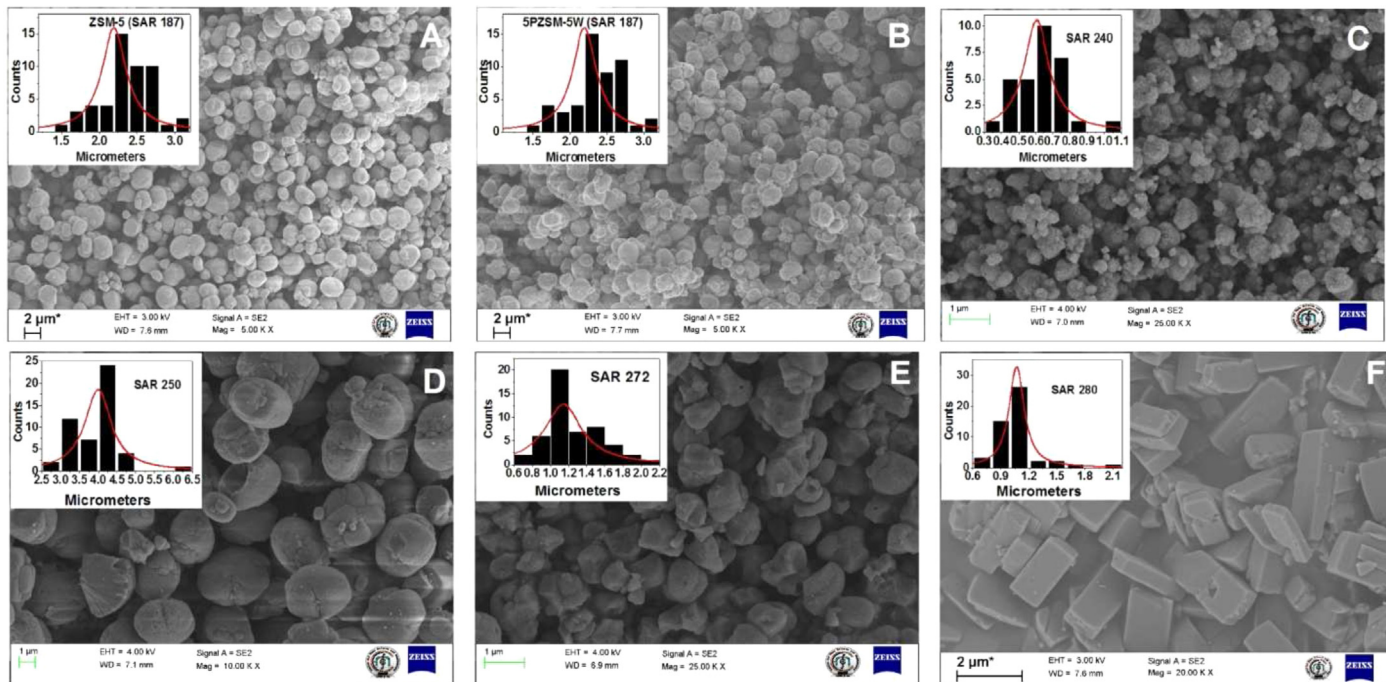


Fig. 4. Scanning electron micrographs of (A) HZSM-5(SAR 187), (B) 5PZSM-5W (SAR 187), (C) HZSM-5(SAR-240), (D) HZSM-5(SAR-250), (E) HZSM-5(SAR-272), (F) HZSM-5(SAR-280).

3.2.1. Effect of silica to alumina ratio of ZSM-5

Silica to alumina ratio (SAR) of zeolite is important for any acid catalyzed reaction as the conversions depend upon the acid site concentration and strength. It is generally observed that, with increase in SAR, amount of acid sites decreases so is the conversion. As the acidity of catalyst decreases, alcohol to olefin side reaction also decreases. This leads to a decrease in coke formation and hence catalyst life increases. Phosphate modification of ZSM-5 not only modifies the acid sites but also narrows the pores. To find the best SAR, 3% P loaded zeolites of different SAR were prepared and studied (Fig. 5A, Table 2). With increase in SAR, conversion decreased as expected, but selectivity for *para* isomer increased progressively from SAR 38 to 407. As added phosphates react with aluminum sites, P/Al increases with increase in SAR with identical 3% P loading. Hence for higher SAR, lower amount of phosphates are sufficient for narrowing of pores and as a result, *para* selectivity increases with increase in SAR. 3PZSM-5W with SAR 187 showed better performance in terms of EB conversion (22.3%) with lesser side products (diethylbenzene selectivity of 85%) and hence this was chosen for further studies.

3.2.2. Optimization of phosphate content

Impregnation of phosphate to ZSM-5 increased the EB conversion as well as selectivity to PDEB (Fig. 5B). Moreover, weaker acid sites generated in 3PZSM-5W ($\text{NH}_3\text{-TPD}$, Fig. 2), decrease the gas formation resulting in increased ethanol utilization towards total DEB. Increase in P from 3 to 5% increased PDEB selectivity from 93 to 98.5% but conversion was almost the same (~22%) for both the catalysts. Further increase in P > 5% increased the selectivity for PDEB but decreased the conversion. This could be due to the diffusion limitation imparted by narrowed zeolite pores even to reactant molecules at higher P concentrations. Due to smaller molecular size, ethanol can easily diffuse into pores and reach active sites resulting in gas forming reactions leading to decreased ethanol utilization towards alkylation. Maximum of 99.5% PDEB selectivity was achieved with 9% P on ZSM-5 (SAR 187) with 9% EB conversion. Considering both conversion and selectivity, optimum concentration of P was 5 wt% which gave 23% conversion with 98.5% PDEB selectivity in 4 h time on stream.

3.2.3. Effect of 2-step phosphate modification

It is shown that phosphates interact with aluminium sites of ZSM-5 and form phosphate islands with increase in phosphate concentration [22]. Modification of ZSM-5 with phosphate was carried out in 2 steps to understand the phosphate and zeolite interaction (Table 3). For this, total phosphates added in 2 steps were kept constant at 5 wt% (as described in experimental section). Phosphate modified catalysts prepared in two steps and in the single step contained similar amount of phosphates (0.7–0.9%) as well as similar acidity (in the range of 0.17–0.22 mmol/g). This is despite the fact that water treatment was carried out in every step to remove water-soluble phosphates. Interestingly, activity and selectivity of different catalysts prepared in two steps (with % P addition; 1+4, 2+3, 3+2) were same with 21% EB conversion with 97% selectivity whereas for single step addition, conversion was 23% with 98% selectivity for PDEB. This shows that, single step addition of phosphates gave marginally better performance than two-step addition.

3.2.4. Effect of temperature

With increase in temperature from 320 to 400 °C, activity of the catalyst increased as expected (Fig. 5C). EB conversion increased from 7.1 to 25% whereas PDEB selectivity remained almost the same (~98%) at all temperatures. However, total DEB selectivity increased from 90.9 to 93.4% as the temperature increased from 320 to 360 °C and it decreased to 84.9% with further increase in temperature to 380 °C. As the temperature was increased from

380 to 400 °C, EB conversion improved by 2% however, DEB selectivity decreased due to higher dealkylation to form benzene. Ethanol utilization towards DEB increased as the temperature was increased upto 380 °C and then remained constant. Hence, 380 °C was optimum temperature with good conversion (23%), high PDEB selectivity (98.5%) and ethanol utilization towards DEB (69.64%).

3.2.5. Effect of reactants mole ratio

Effect of mole ratio was studied at 380 °C, WHSV of 3 h⁻¹ and H₂/reactants mole ratio of 2 (Fig. 5D). Limiting reactant, ethanol conversion was invariably >99% in all the experiments. With decrease in EB to ethanol mole ratio from 8:1 to 1:1, the conversion of EB increased from 17.2 to 33.5%. With increase in concentration of alkylating agent, total DEB increased from 72.6 to 90.8% instead of heavy aromatics. This could be due to the restricted pore size of PZSM-5, which avoids the formation of bulkier products inside the channels. Even though the conversion of EB increased with increase in alkylating agent, it did not increase proportionately with respect to increase in ethanol concentration in the feed because more amount of ethanol converted into gaseous products at higher ethanol concentrations (Table S2). Due to this, ethanol utilization towards DEB decreased substantially from 77.3 to 29.6% with decrease in EB:Ethanol from 8:1 to 1:1. Optimum mole ratio was found to be 4:1, considering good conversion (22.8%) and high ethanol utilization (69.6%).

3.2.6. Effect of space velocity

Weight hourly space velocity (WHSV) gives a correlation between throughput and contact time. With increase in WHSV from 1 to 10 h⁻¹, conversion progressively decreased from 23.9 to 12.5% (Fig. 5E) due to decrease in effective contact time of reactants with the catalyst. At lower WHSV, the side product formation was higher whereas at higher WHSV side products decreased with improvement in total DEB formation. At WHSV = 1 h⁻¹, conversion was 23.9% and DEB selectivity was 77%, whereas at WHSV = 3 h⁻¹ conversion decreased marginally to 22.8% but total DEB increased considerably (85.3%). With further increase in WHSV from 3 to 10 h⁻¹, conversion of EB decreased progressively whereas DEB selectivity improved only marginally. Considering both conversion and selectivities for DEB and PDEB, WHSV of 3 h⁻¹ was chosen as the optimum space velocity.

3.2.7. Effect of Hydrogen

Effect of carrier gas H₂ on the catalyst performance was studied by varying H₂ to reactants mole ratio (Fig. 5F). Without carrier gas (H₂/reactant = 0), dehydration of ethanol predominated over the alkylation forming high amount of gaseous side products. Due to this, the conversion without carrier gas was low (16.7%) with total DEB of 90%. With the introduction of hydrogen as carrier gas (H₂: Reactants = 1), conversion increased to 21% whereas total DEB decreased to 84.0%. With further increase in hydrogen flow of H₂: Reactants = 2, there was marginal variation in conversion and DEB (22.8% and 85.3% respectively). With further increase in the hydrogen flow (H₂: Reactant = 4), conversion and DEB selectivity decreased considerably to 19.8% and 82.5% respectively. Selectivity towards PDEB was constant (~98%) at different carrier gas concentrations in the feed and for further studies were carried out with H₂: Reactant = 2.

Interestingly, PDEB selectivity in the mixture of DEB was very high and remained almost constant (98–99%) under various reaction conditions such as temperature, reactants mole ratio, space velocity and carrier gas concentration in the feed. This suggests that high selectivity achieved for PDEB is independent of operating parameters and truly due to shape selectivity obtained by phosphate modification of ZSM-5 catalyst.

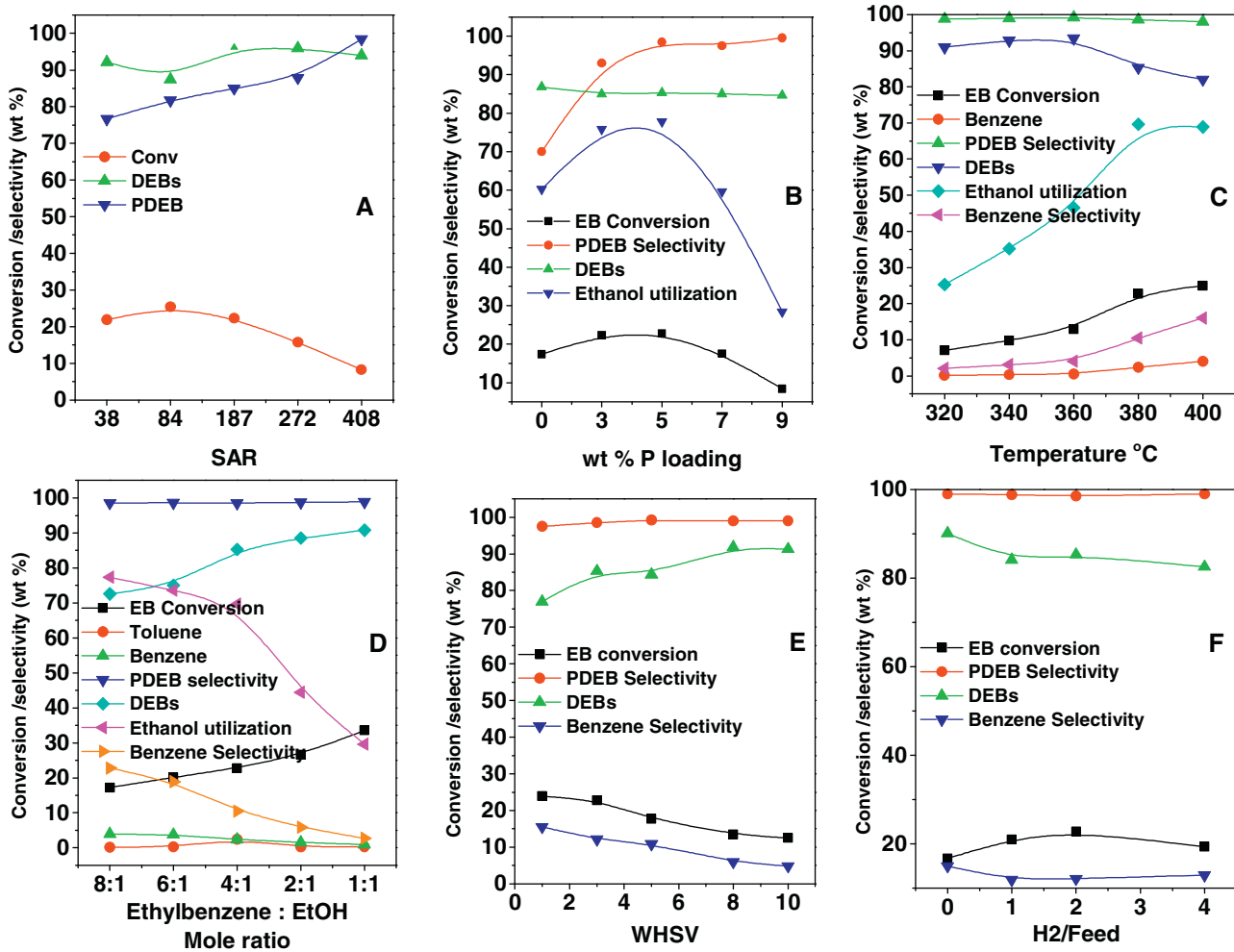


Fig. 5. (A) Effect of P modification on ZSM-5 with different SAR; (B) Optimization of P content on ZSM-5 (SAR 187) (conditions for (A) and (B)): temperature = 380 °C WHSV = 3 h⁻¹, catalyst weight = 2 g, H₂: reactants = 2, ethylbenzene:ethanol = 4:1, time = 4 h; (C) effect of temperature (conditions: WHSV = 3 h⁻¹, catalyst weight = 2 g, H₂: reactants = 2, ethylbenzene:ethanol = 4:1, time = 4 h); (D) effect of reactant mole ratio (conditions: temperature = 380 °C WHSV = 3 h⁻¹, catalyst weight = 2 g, H₂: reactants = 2, time = 4 h); (E) Effect of space velocity (conditions: temperature = 380 °C, catalyst weight = 2 g, H₂: reactants = 2, ethylbenzene:ethanol = 4:1, time = 4 h); (F) effect of hydrogen as carrier gas (conditions: temperature = 380 °C WHSV = 3 h⁻¹, catalyst weight = 2 g, ethylbenzene:ethanol = 4:1, time = 4 h).

3.2.8. Effect of crystal size and morphology

Study on the effect of zeolite crystal size is important as it gives information on the mechanism of shape selectivity of the catalyst [36]. Crystal size has a direct correlation with selectivity to *para* isomer formed during aromatic substitution reactions. For a catalyst with larger crystal size, the selectivity of *para*-isomer is greater than that of selectivity in thermodynamic equilibrium mixture of isomers. It could be observed from optimization of reaction parameters that PDEB selectivity is not affected by the reaction conditions and EB conversion levels because the selectivity for PDEB is the property of shape selectivity of phosphate modified ZSM-5. Hence, the difference in conversion levels obtained for different crystal sizes could be ignored while correlating crystal size with PDEB selectivity. Silica extrudates of three different crystal sizes of ZSM-5 with similar SAR (similar acidity) were studied for ethylation of ethylbenzene under the same reaction conditions (Table 1, Fig. 4). Unmodified HZSM-5 catalysts with different crystal sizes were compared to understand the size effect. It is observed that as the average crystal size increased from 0.3 to 1.2 μm, EB conversion decreased from 35.6 to 16.7% whereas PDEB selectivity enhanced from 38.6 to 66.1%. With crystal size of 1.1 μm and cuboid morphology did not change the conversion and selectivity appreciably (16.3% conversion and 62.7% selectivity). For ZSM-5 with large crystals (Avg. crystal size = 3.9 μm), conversion increased to

25.5% whereas PDEB selectivity decreased marginally (61.4%). For zeolite with smaller crystal size, product can diffuse easily without much diffusion barrier and hence the activity of the catalyst was high. It is found that benzene formation due to dealkylation of EB was higher for unmodified ZSM-5 with small and large crystals. Dealkylation decreased marginally after phosphate modification but benzene still remained as major side product. At lower concentration of phosphates (2% P), PDEB selectivity increased with increase in crystal size. At higher concentrations (5% P), small crystal size (0.63 μm) attained 88.3% PDEB selectivity and it increased to 91.5% for 1.1 μm with cuboid shape. *Para* isomer selectivity was maximum for 1.2 μm with irregular shape and 3.9 μm size crystals (~98%). Difference in *para* selectivity for 1.1 μm size crystals could be due to their different morphologies and marginally less conversion due to marginal difference in SAR. Lower PDEB selectivity for 0.63 μm size catalyst suggests that more phosphates are needed for smaller crystal size zeolite to achieve similar PDEB selectivity comparable with bigger crystal size zeolites. This could be due to reduced path length for zeolite with small crystal size, which increases the number of zeolite channels per unit volume compared with zeolite with bigger crystals. At lower concentration of phosphates, all the isomers are formed over the catalyst but due to a diffusion barrier imparted by phosphates results in the increased PDEB selectivity. Phosphates in the micropores of ZSM-5 not only

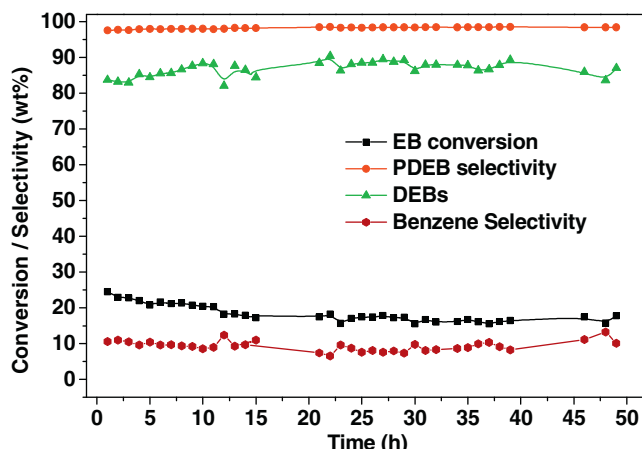


Fig. 6. Time on stream under optimized reaction parameters (*conditions*: temperature = 380 °C WHSV = 3 h⁻¹, catalyst weight = 2 g, H₂: reactants = 2, ethylbenzene:ethanol = 4:1).

increase the diffusion barrier but also decrease the pore volume (Table S1). Decrease in pore volume reduces the formation of transition state of bulkier *m*-DEB and *o*-DEB and hence low selectivities for *m* and *o*-DEB were observed at higher phosphate concentrations. These results show that, at lower phosphate concentrations, phosphate modification imparts diffusion barrier to the formed isomers and hence mechanism of product shape selectivity could be proposed. However, at higher phosphate concentrations, restricted transition state mechanism is also possible. It is reported elsewhere that product shape selectivity depends on the length of inter crystalline diffusion path and hence the measurable selectivity effects decrease with decrease in crystal size. If restricted transition state shape selectivity is operative, the measurable selectivity will be independent of the crystal size [36].

3.2.9. Time on stream (TOS)

TOS was carried out under optimized conditions of 380 °C, EB:Ethanol mole ratio 4:1, WHSV = 3 h⁻¹ and H₂: Reactant = 2 (Fig. 6). Catalyst initially showed high EB conversion of 22.5% after 4 h and then decreased gradually to 20% in 11 h TOS. The conversion decreased to 18.2% after 22 h and then remained constant at ~18% till 50 h TOS without any further deactivation. Marginal increase in PDEB selectivity from 97.7 to 98.4% during 50 h TOS could be attributed to small amount of coke formed during the reaction. Coke content after 50 h reaction was found to be 2.9%. Catalyst was regenerated after the reaction and tested under the same conditions for 12 h (Fig. S8). The recycled catalyst showed 19% EB conversion after 12 h reaction, about 1% lower than that of fresh catalyst. There was a marginal increase in DEB selectivity by 3% after regeneration (88–91%) whereas PDEB selectivity remained almost the same (98%). Regained activity and PDEB selectivity during catalyst recycle suggests that phosphate modification of ZSM-5 remained intact during 50 h reaction.

4. Conclusions

Selective synthesis of *p*-diethylbenzene from alkylation of ethylbenzene is an important, industrially applicable reaction. Impregnation of phosphates on ZSM-5 effected the pore narrowing and enhanced the shape selectivity towards smallest monoalkylated isomer, *p*-diethylbenzene with good conversion. Study on zeolite crystal size showed that at lower phosphate concentrations, phosphate modification imparts diffusion barrier to the formed isomers and hence mechanism of product shape selectivity is proposed. However, at higher phosphate concentrations,

restricted transition state mechanism is also possible. Acid site density of the catalyst is important as phosphates react with Al and increase diffusion barrier. ZSM-5 with SAR 187 was found to contain optimum acidity for phosphate modification to achieve good conversion and high selectivity for *p*-diethylbenzene. With increase in phosphate loading, *para* selectivity increased and 5% P (as oxide) on ZSM-5 was found to be optimum loading with good conversion (22.8%) and high PDEB selectivity (98.5%). Single step phosphate modification was better than two-step modification to achieve high activity and selectivity for *p*-diethylbenzene. High and unchanged *p*-diethylbenzene selectivity in the mixture of diethylbenzenes (98–99%) under various reaction conditions suggested that high selectivity achieved for *p*-diethylbenzene is independent of operating parameters and truly due to shape selectivity obtained by phosphate modification of ZSM-5 catalyst. Under optimized reaction conditions, catalyst showed good stability towards deactivation during 50 h of time on stream with minimum coke deposition.

Acknowledgements

HLJ acknowledges Admar Mutt Education Foundation (AMEF), Bangalore for a fellowship and Manipal University, India for permitting this research as a part of the Ph.D. programme. Authors gratefully thank Sophisticated Instrument Facility, Indian Institute of Science, Bangalore for collecting MAS NMR experimental data and Centre for Nanoscience and Engineering, Indian Institute of Science, Bangalore for SEM images.

Appendix A. Supplementary data

Supplementary material related to this article can be found, in the online version, at <http://dx.doi.org/10.1016/j.apcata.2014.07.006>.

References

- [1] K. Tanabe, Appl. Catal. A 181 (1999) 399–434.
- [2] A.B. Halgeri, J. Das, Catal. Today 73 (2002) 65–73.
- [3] Y.S. Bhat, J. Das, A.B. Halgeri, J. Catal. 155 (1995) 154–157.
- [4] J. Das, Y.S. Bhat, A.B. Halgeri, Ind. Eng. Chem. Res. 32 (1993) 2525–2529.
- [5] G. Kamalakar, S.J. Kulkarni, K.V. Raghavan, S. Unnikrishnan, A.B. Halgeri, J. Mol. Catal. A 149 (1998) 283–288.
- [6] T. Hibino, M. Niwa, Y. Murakami, J. Catal. 128 (1991) 551–558.
- [7] D.V. Vu, M. Miyamoto, N. Nishiyama, Y. Egashira, K. Ueyama, Catal. Lett. 127 (2009) 233–238.
- [8] Y. Sugi, Y. Kubota, K. Komura, N. Sugiyama, M. Hayashia, J.H. Kimb, G. Seob, Appl. Catal. A 299 (2006) 157–166.
- [9] W.W. Kaeding, J. Catal. 120 (1989) 409–412.
- [10] W.W. Kaeding, L.B. Young, C.C. Chu, J. Catal. 89 (1984) 267–273.
- [11] W.W. Kaeding, J. Catal. 95 (1985) 512–519.
- [12] W.W. Kaeding, S.A. Butter, J. Catal. 61 (1980) 155–164.
- [13] A. Corma, V. Fornes, W. Kolodziejski, L.J. Martineztrigero, J. Catal. 145 (1994) 27–36.
- [14] G. Lischke, R. Eckelt, H.G. Jerschewitz, B. Parltitz, E. Schreier, T.W. Stork, B. Zibrowius, G. Ohlmann, J. Catal. 132 (1991) 229–243.
- [15] T. Blasco, A. Corma, J. Martineztrigero, J. Catal. 237 (2006) 267–277.
- [16] W.W. Kaeding, C. Chu, L.B. Young, B. Weinstein, S.A. Butter, J. Catal. 67 (1981) 159–174.
- [17] L.B. Young, S.A. Butter, W.W. Kaeding, J. Catal. 76 (1982) 418–432.
- [18] K. Chandawar, S. Kulkarni, P. Ratnasamy, Appl. Catal. 4 (1982) 287–295.
- [19] A.K. Gosh, N. Kulkarni, P. Harvey, US Patent 7713898 B2 (2010) to SABIC.
- [20] M. Göhlich, W. Reschetilowski, S. Paasch, Micropor. Mesopor. Mater. 142 (2011) 178–183.
- [21] D. Liu, W.C. Choi, C.W. Lee, N.Y. Kang, Y.J. Lee, C.-H. Shin, Y.K. Park, Catal. Today 164 (2011) 154–157.
- [22] H.L. Janardhan, G.V. Shanbhag, A.B. Halgeri, Appl. Catal. A 471 (2014) 12–18.
- [23] W. Xiangsheng, W. Guiru, G. Hongchen, W. Xueqin, in: H. Chon, S.-K. Ihm, Y.S. Uh (Eds.), Stud. Surf. Sci. Catal. 105 (1997) 1357–1364.
- [24] K.U. Nandhini, B. Arabindoo, M. Palanichamy, V. Murugesan, Micropor. Mesopor. Mater. 81 (2005) 59–71.
- [25] K.J.A. Raj, M.S. Meenakshi, V.R. Vijayaraghavan, J. Mol. Catal. A 270 (2007) 195–200.
- [26] A.B. Halgeri, J. Das Catal. Today 73 (2002) 65–73.

- [27] Y. Sugi, Y. Kubota, K. Komura, N. Sugiyama, M. Hayashi, J.H. Kim, in: J. Cejka, N. Zilkova, P. Nachtigall (Eds.) *Stud. Surf. Sci. Catal.* 158 (2005) 1279–1286.
- [28] Y.S. Bhat, J. Das, A.B. Halgeri, *Appl. Catal. A* 115 (1994) 257–267.
- [29] J. Das, A.B. Halgeri, *Catal. Surv. Asia* 7 (2003) 3–9.
- [30] Y.S. Bhat, A.B. Halgeri, *Appl. Catal.* 101 (1993) 95–104.
- [31] Y.S. Bhat, J. Das, A.B. Halgeri, *Appl. Catal. A* 122 (1995) 161–168.
- [32] S.A. Moya, M. Escudey, *J. Chem. Soc. Chem. Commun.* (1994) 1829–1830.
- [33] C. Warwick, A. Guerreiro, A. Soares, *Biosens. Bioelectron.* 41 (2013) 1–11.
- [34] M. Derewinski, P. Sarv, X. Sun, S. Müller, A.C. Van Veen, J.A. Lercher, *J. Phys. Chem. C* 118 (2014) 6122–6131.
- [35] H.E. van der Bij, L.R. Aramburo, B. Arstad, J.J. Dynes, J.B. Wang, M. Weckhuysen, *ChemPhysChem* 15 (2014) 283–292.
- [36] Y. Traa, S. Sealy, J. Weitkamp, in: H.G. Karge, J. Weitkamp (Eds.), *Molecular Sieves, Characterization II*, Springer, Berlin, Heidelberg, 2007, pp. 103–154.
- [37] J.A. Lercher, G. Rumpfmayr, *Appl. Catal.* 25 (1986) 215–222.
- [38] N. Xue, R. Olindo, J.A. Lercher, *J. Phys. Chem. C* 114 (2010) 15763–15770.